Chinese Chemical Letters 37 (2026) 112122

Contents lists available at ScienceDirect

Chinese Chemical Letters

journal homepage: www.elsevier.com/locate/cclet

Polymerizable deep eutectic solvent–based gels with recyclability and self-healing for low-temperature wearable sensing

Yinzhou Guo[a,1], Yuanyuan Chen[a,1], Min Zhang[c], Chenhui Cui[a], Xiaoqing Ming[a], Zhang Qiang[a], Jiao Jiao[a], Yilong Cheng[a,b], Zhishen Ge[a,b], Yanfeng Zhang[a,b,*]

[a] School of Chemistry, Xi'an Key Laboratory of Sustainable Polymer Materials, Engineering Research Center of Energy Storage Materials and Devices, Ministry of Education, Institute of New Concept Sensors and Molecular Materials (INCSMM), Xi'an Jiaotong University, Xi'an 710049, China
[b] State Key Laboratory of Fluorine & Nitrogen Chemicals, Xi'an 710049, China
[c] Northwest Rubber & Plastic Research and Design Institute Co., Ltd., Xianyang 712023, China

ARTICLE INFO

Article history:
Received 15 September 2025
Revised 13 November 2025
Accepted 14 November 2025
Available online 14 November 2025

Keywords:
Polymerizable deep eutectic solvent (PDES)
Recyclable gel
Self-healing material
Low-temperature sensing
Wearable electronics

ABSTRACT

Flexible wearable sensors require conductive elastomers that combine sustainability, durability, and reliable low-temperature performance. However, conventional hydrogels suffer from dehydration and freezing, while ionogels face challenges of leakage, high cost, and poor recyclability. Here, we introduce a novel polymerizable deep eutectic solvent (PDES) system based on natural lipoic acid and imidazolium derivatives, which serves as the foundation for constructing recyclable polymeric dynamic eutectic gels (PDDEGs). The PDES not only provides high ionic mobility and antifreeze capacity but also enables covalent crosslinking to form a robust yet dynamic polymeric network. Through synergistic hydrogen bonding, ionic conduction, and reversible zirconium coordination, PDDEGs achieve high stretchability, toughness, and strong adhesion. More importantly, they exhibit remarkable recyclability, efficient self-healing, and thermal remoldability, allowing solvent-free reprocessing, structural repair, and adaptive reshaping without performance loss. The gels remain flexible and conductive at −20 °C and function as reliable strain sensors with high sensitivity, fast response, and long-term durability in monitoring complex human motions. By combining a new class of polymerizable eutectic solvents with dynamic crosslinking, this work establishes a sustainable platform for next-generation wearable electronics capable of operating in extreme environments.

© 2026 Published by Elsevier B.V. on behalf of Chinese Chemical Society and Institute of Materia Medica, Chinese Academy of Medical Sciences.

Flexible wearable sensors can convert mechanical deformation, temperature, and humidity into electrical signals [1–6]. They have found widespread applications in soft robotics, human motion detection, health monitoring, and electronic skin [7–11]. Conductive elastomers play a key role in these devices due to their stretchability, transparency, and electrical conductivity [12–14]. Among them, hydrogels and ionogels are the most commonly used systems. Hydrogels offer flexibility, biocompatibility, and ionic conductivity. However, they suffer from water loss and freezing at low temperatures [15–18]. This limitation leads to degraded performance or even complete failure. Ionogels, composed of nonvolatile ionic liquids, can circumvent water evaporation and freezing issues. Yet, they are prone to liquid leakage, involve complex and costly synthesis, and may pose environmental risks [19–21]. These drawbacks make conventional gels inadequate for reliable sensing under low-temperature conditions.

Deep eutectic solvents (DESs) have emerged as green alternatives. They are composed of a hydrogen bond donor (HBD) and a hydrogen bond acceptor (HBA) [22–26]. DESs share many properties with ionic liquids but are cheaper, easier to prepare, and more biocompatible. DES-based gels are therefore considered sustainable conductive elastomers [27–29]. Choline chloride (ChCl)-based gels are biodegradable and low-cost but show poor ionic mobility and weak antifreeze ability [30–32]. Non-degradable polymer-supported DES gels exhibit high mechanical strength but suffer from poor recyclability and limited sustainability [33–35]. To overcome this trade-off, recyclable eutectic gels must be developed that integrate sustainability, ionic conductivity, mechanical resilience, and antifreeze performance. A promising approach is to construct gels from natural small molecules as the matrix combined with conductive small molecules [36,37]. This strategy enables the formation of eutectic networks that couple sustainability

* Corresponding author.
E-mail address: yanfengzhang@xjtu.edu.cn (Y. Zhang).
[1] These authors contributed equally to this work.

https://doi.org/10.1016/j.cclet.2025.112122
1001-8417/© 2026 Published by Elsevier B.V. on behalf of Chinese Chemical Society and Institute of Materia Medica, Chinese Academy of Medical Sciences.

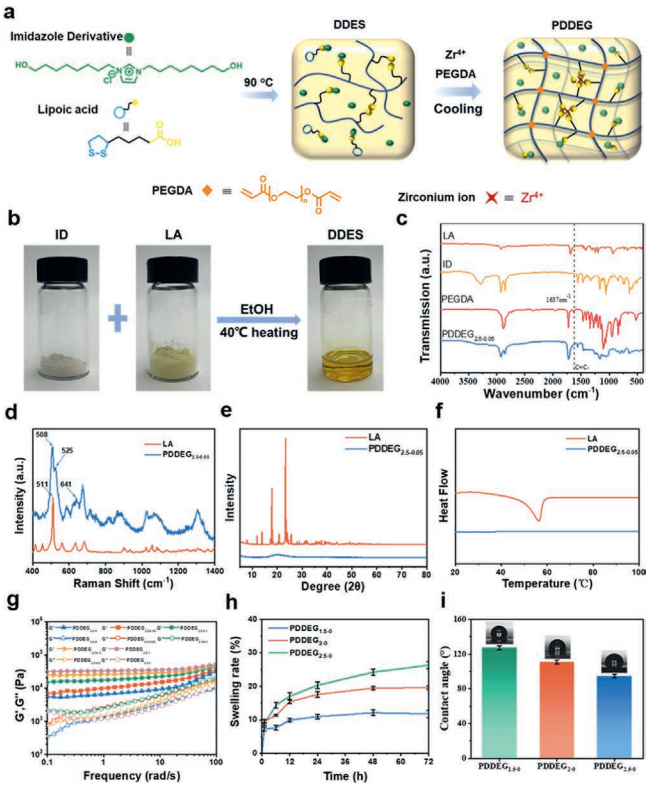


Fig. 1. (a) Schematic diagram of the preparation of recyclable polymeric dynamic eutectic gel. (b) Photos of the preparation of lipoic acid-imidazole derivative DES. (c) FT-IR spectra of LA, ID, PEGDA and $PDDEG_{2.5-0.05}$. (d) Raman spectra of LA and $PDDEG_{2.5-0.05}$. (e) XRD pattern of LA and $PDDEG_{2.5-0.05}$. (f) DSC thermograms of LA and $PDDEG_{2.5-0.05}$. (g) The change of moduli *versus* angular frequency (0.1–100 rad/s) for PDDEGs. (h) Swelling rate of PDDEG with different eutectic ratios (1.5, 2, 2.5). (i) Water contact angles of PDDEG with different eutectic ratios (1.5, 2, 2.5). Data are presented as mean ± standard deviation (SD) ($n = 5$).

with ionic mobility and antifreeze properties, thereby expanding the potential of low-temperature wearable sensors.

In this work, we present a polymerizable deep eutectic solvent (PDES) system derived from natural lipoic acid and imidazolium derivatives. This system serves as the basis for constructing recyclable polymeric dynamic eutectic gels (PDDEGs). The PDES provides high ionic mobility and intrinsic antifreeze capability, while polymerization introduces a robust yet dynamic network. Multiple interactions, including hydrogen bonding, ionic conduction, and reversible zirconium coordination, endow PDDEGs with high stretchability, toughness, and strong adhesion. The gels further exhibit efficient self-healing, remarkable recyclability, and thermal remoldability, enabling solvent-free reprocessing and adaptive reshaping without performance loss. Notably, they remain flexible and conductive at −20 °C and function as reliable strain sensors with high sensitivity, fast response, and long-term stability in complex motion monitoring. By integrating a new class of polymerizable eutectic solvents with dynamic crosslinking, this study establishes a sustainable and versatile platform for next-generation wearable electronics in extreme environments.

The fabrication process of PDDEG is illustrated in Fig. 1a. Briefly, lipoic acid (LA) and imidazolium derivative (ID) were first dissolved in EtOH, and most of the solvent was removed by rotary evaporation. The mixture was then heated at 40 °C for 20 min to form dynamic deep eutectic solvents (DDES), in which ID acted as a HBA and LA served as a hydrogen bond donor (Fig. 1b). Subsequently, polyethylene glycol diacrylate (PEGDA) and zirconium ions were introduced to copolymerize with LA, and the mixture was stirred for 10 min at 90 °C. The resulting liquid precursor was poured into a mold and cured at 40 °C for 24 h to yield PDDEGs. Here, "$PDDEG_{x-y}$" refers to polymeric dynamic deep eutectic gels prepared with different molar ratios of LA to ID, where x represents the LA:ID ratio (1.5, 2.0, 2.5), and y denotes the zirconium ion concentration (0, 0.05, 0.1, 0.5 or 1 wt%). For example, $PDDEG_{2.5-0.05}$ corresponds to a gel synthesized with an LA:ID ratio of 2.5:1 and 0.05 wt% Zr^{4+}. The imidazolium derivative was deliberately selected as the HBA because its high polarity and strong affinity toward the carboxyl groups of LA promote the formation of a stable eutectic phase with enhanced ionic conductivity. The LA/ID molar ratio was systematically tuned (1.5, 2.0, and 2.5) to control the hydrogen-bond density within the eutectic network, as stable deep eutectic systems typically form only within specific donor–acceptor proportions. Therefore, the three ratios of 1.5, 2, and 2.5 that can form low eutectic solvents were selected for research.

The chemical structure of the obtained gels was verified by spectroscopic characterization. In the Fourier transform infrared (FT-IR) spectrum (Fig. 1c and Fig. S3 in Supporting information), the disappearance of peaks at 1635 and 1620 cm^{-1} (C=C) confirmed the covalent crosslinking between LA and PEGDA. Raman spectra further supported this observation: in $PDDEG_{2.5-0.05}$ (Fig. 1d), the single S–S stretching vibration at 511 cm^{-1} in LA split into two peaks at 508 and 525 cm^{-1}, indicating the ring-opening polymerization of LA. Additionally, the appearance of a new band at 641 cm^{-1}, corresponding to C–S stretching, provided further evidence for the formation of covalent crosslinks between LA and PEGDA [38]. X-ray diffraction (XRD) analysis also confirmed the amorphous nature of the polymer network (Fig. 1e). No distinct diffraction peaks were observed in $PDDEG_{2.5-0.05}$, demonstrating the successful construction and structural stability of the poly(LA)-based network. Moreover, the rapid decomposition temperature of the resulting PDDEGs (319 °C) is found to be slightly higher than that of LA by TGA (Fig. S6 in Supporting information), showing a higher thermal stability. The absence of the characteristic melting temperature of LA (58 °C) in differential scanning calorimetry (DSC) thermograms indicates a complete depletion of the monomer (Fig. 1f).

To verify the stability of PDDEGs, rheological tests were conducted to evaluate the dependence of its storage modulus (G') and loss modulus (G'') on frequency and strain. As shown in Fig. 1g and Fig. S7 (Supporting information), G' remained higher than G'' over the entire testing range, demonstrating the dominant elastic nature and structural integrity of the gel network. The hydrophobicity of PDDEGs were further examined by water swelling and contact angle measurements. As shown in Figs. 1h and i, increasing the lipoic acid content resulted in a higher swelling ratio and a smaller contact angle, which decreased from 125° to 89°. This behavior is attributed to the increase of lipoic acid, which leads to an increase in carboxyl groups in PDDEGs, thereby increasing the hydrophilicity of the overall material, resulting in an increase in the swelling ratio and a decrease in the hydrophobic angle. To investigate the morphology of the eutectic gel, we used scanning electron microscopy (SEM) to observe the surface of PDDEG (Fig. S8 in Supporting information). The images revealed a smooth surface, indicating that the DES remained stably bound within the gel even after freeze-drying, demonstrating the stability of the gel material at low temperatures and pressures.

The mechanical properties of the lipoic acid–imidazolium deep eutectic gels were systematically investigated using a universal tensile testing machine. Figs. 2a–c show the tensile properties of the eutectic gels with different lipoic acid–imidazolium ratios (1.5:1; 2.0:1 and 2.5:1). The tensile properties of cocrystal gels with varying lipoic acid-imidazolium ratios exhibited a clear composition-dependent trend. At low lipoic acid content, the gels exhibited a break stress of ~17.9 kPa and an elongation at break of ~980 %, reflecting high flexibility and segmental mobility. With

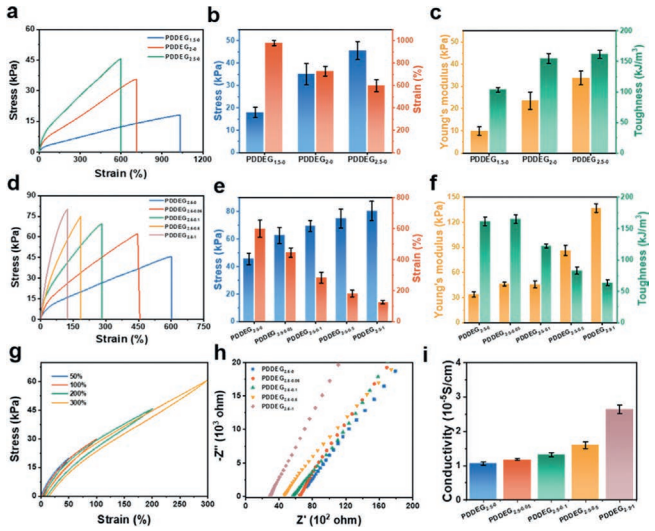


Fig. 2. (a) Stress-strain curves of PDDEGs with different deep eutectic ratios. (b) Breaking stress and strain of PDDEGs with different deep eutectic ratios. (c) Young's modulus and toughness of PDDEGs with different deep eutectic ratios. (d) Stress-strain curves of $PDDEG_{2.5}$s with different Zr^{4+} contents. (e) Breaking stress and strain of $PDDEG_{2.5}$s with different Zr^{4+} contents. (f) Young's modulus and toughness of $PDDEG_{2.5}$s with different Zr^{4+} contents. (g) Cyclic tensile curves of the $PDDEG_{2.5-0.05}$ with different strains. (h) Electrochemical impedance spectroscopy plots of $PDDEG_{2.5}$s with different Zr^{4+} contents. (i) Ionic conductivities of $PDDEG_{2.5}$s with different Zr^{4+} contents. Error bars represent the SD ($n = 5$).

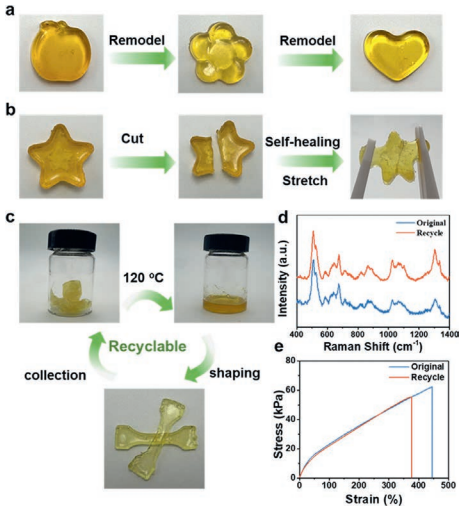


Fig. 3. (a) Photographs of the remodeled property of $PDDEG_{2.5-0.05}$ under 70 °C. (b) Photographs of the self-healing process for $PDDEG_{2.5-0.05}$. (c) The recycling process of $PDDEG_{2.5-0.05}$. (d) Raman spectra of original and recycled $PDDEG_{2.5-0.05}$. (e) Stress-strain curves of original and recycled $PDDEG_{2.5-0.05}$.

increasing lipoic acid ratios, the break stress rose to ~45.6 kPa, while the elongation at break decreased to approximately 600 %. Concomitantly, the Young's modulus increased from approximately 9.9 kPa to approximately 33.8 kPa, and the toughness initially increased from ~103.7 kJ/m^3 to a maximum of ~161.7 kJ/m^3 at an intermediate salt ratio. This trend suggests that moderate hydrogen bonding crosslinking optimizes energy dissipation while maintaining ductility by providing sufficient reversible sacrificial bonds.

Considering the comprehensive properties of $PDDEG_{2.5}$, such as mechanical properties and hydrophilicity, it was selected as the matrix to study the effect of different zirconium ion contents on the mechanical properties of eutectic gel. The results are shown in Figs. 2d–f. resulting in markedly increased strength and stiffness compared with salt-only gels. As the Zr^{4+} content rises, the fracture stress increases from 45.6 kPa to 80.5 kPa, and the modulus climbs from 33.8 kPa to 137.1 kPa, while the fracture strain decreases sharply from 600 % to 126 %, indicating that Zr^{4+} act as strong coordination centers that increase the effective crosslink density and reinforce the network. The toughness exhibits a nonlinear dependence on Zr^{4+} concentration: it initially rises to a maximum of 165.2 kJ/m^3 at low-to-moderate Zr^{4+} levels due to the synergistic energy dissipation from coexisting ionic and coordination interactions, but declines sharply to 63.7 kJ/m^3 at high Zr^{4+} content, where excessive crosslinking reduces ductility and limits the gel's capacity to absorb energy.

To further evaluate its elasticity, $PDDEG_{2.5-0.05}$ was subjected to loading–unloading tests. Single-cycle curves at different strains (50 %, 100 %, 200 %, and 300 %) during continuous stretching (Fig. 2g) show a pronounced hysteresis loop, indicating effective dissipation of strain energy through the rupture of dynamic hydrogen bonds. The fatigue resistance and mechanical durability were further assessed *via* 30 consecutive loading–unloading cycles (Fig. S9 in Supporting information). The hysteresis loop gradually decreased over repeated cycles, suggesting partial, yet incomplete, recovery of the polymer network structure after each stretch–retraction process. After 30 cycles, $PDDEG_{2.5-0.05}$ exhibited a residual strain of 24 % while retaining 85 % of its initial stress, demonstrating excellent resilience and long-term mechanical durability.

In addition to mechanical properties, the effect of the ratios of deep eutectic solution and Zr^{4+} content on the electrical conductivity of PDDEGs was also systematically investigated. As shown in Figs. 2h and i and Figs. S10 and S11 (Supporting information), as the Zr^{4+} content increases from 0 to 1 %, the electrical conductivity increases from 1.1×10^{-5} S/cm to 2.7×10^{-5} S/cm. Therefore, the effect of zirconium ions on electrical conductivity is positive. Zirconium ions can form coordination bonds with carboxylates. As the addition level increases, not only can the mechanical properties of the eutectic gel be manipulated, but the electrical conductivity of the material can also be simultaneously improved.

To evaluate the remodelability and self-healing behavior, plasticity and healing tests were performed on the PDDEGs. After softening at 70 °C the material could be molded into diverse geometries (apple, flower, heart) and, upon cooling to room temperature, the reshaped forms remained stable over extended periods (Fig. 3a). This reversible reshaping is driven by thermal disruption of dynamic hydrogen bonds at elevated temperature, which increases polymer chain mobility, followed by hydrogen-bond reformation on cooling that locks in the new configuration and restores mechanical integrity.

The self-healing capability was assessed using a flower-shaped sample that was cut, precisely reassembled at the fracture interface and heat at 100 °C for 3 min (Fig. 3b). During thermal treatment, reversible hydrogen bonds and a fraction of disulfide linkages are activated, promoting chain diffusion, interfacial entanglement and dynamic bond reorganization; subsequent cooling reconstructs the dynamic crosslinked network and recovers the sample's structural integrity. The healed specimen withstood tensile loading applied by tweezers without rupture, confirming effective mechanical repair. Real-time resistance monitoring over cut–repair cycles (Fig. S12 in Supporting information) showed that the electrical resistance sharply increased upon cutting and quickly returned to its initial value after rejoining, indicating rapid restoration of the conductive pathway. This fast electrical and mechanical recovery is primarily governed by thermally activated hydrogen-bond dissociation and reformation, which promote chain mobility and interfacial reconnection within minutes. In contrast, disulfide exchange, although also triggered by heat, occurs more gradually. Only a limited number of disulfide bonds undergo cleavage and recombi-

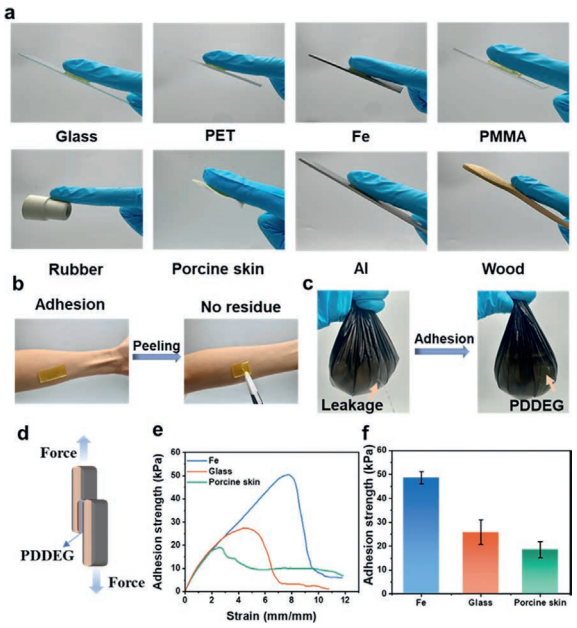


Fig. 4. (a) Photos of the adhesion of $PDDEG_{2.5-0.05}$ on different material surfaces in air. (b) Photos of $PDDEG_{2.5-0.05}$ adhesion and peeling on human skin. (c) Photo of mending a leaking hole with $PDDEG_{2.5-0.05}$. (d) Schematic diagram of lap shear test. (e) Representing curves of the lap-shear strength for $PDDEG_{2.5-0.05}$ with various substrates in the air. (f) The adhesion strength of $PDDEG_{2.5-0.05}$ with various substrates in air. Data are presented as mean ± SD ($n = 5$).

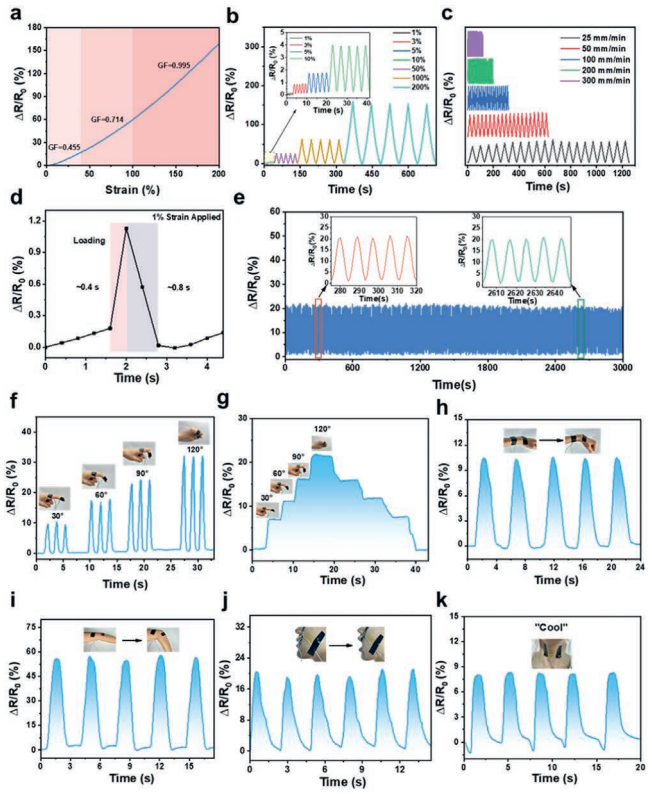


Fig. 5. (a) Gauge factor of the $PDDEG_{2.5-0.05}$ with segmented strain regions. (b) Relative resistance changes of the $PDDEG_{2.5-0.05}$ under various strains. (c) Relative resistance variation of the $PDDEG_{2.5-0.05}$ under different tensile speeds at 50% strain. (d) Response time of $PDDEG_{2.5-0.05}$ under 1% strain applied. (e) Relative resistance changes of the $PDDEG_{2.5-0.05}$ were tested for 300 loading-unloading cycles under 30% strain, the inset is an enlarged view of the cyclic stretch. $PDDEG_{2.5-0.05}$ as a strain sensor for real-time monitoring of human motion at room temperature: (f, g) finger bending at different angles, (h) wrist extension and flexion, (i) elbow extension and flexion, (j) mouth opening, (k) the action of saying "Cool".

nation during short heating, which assists interfacial healing while preserving the overall shape stability of the gel. The synergistic mechanism of rapid hydrogen bond recombination and slower disulfide bond exchange endows PDDEGs with excellent rapid self-repairability and structural stability during the repair process.

Recyclability is a key attribute for sustainable polymer systems; therefore, solvent-free thermal reprocessing of PDDEGs was investigated. $PDDEG_{2.5-005}$ was converted into a flowable molten state by heating at 120 °C for 20 min and subsequently reformed into a solid gel upon cooling (Fig. 3c). Raman spectra of the original and recycled specimens showed no significant changes in peak positions or intensities, indicating preservation of the chemical structure after thermal reprocessing (Fig. 3d). Mechanical testing corroborated this structural retention: the fracture stress of the recycled sample remained 55.6 kPa (Fig. 3e). The observed recyclability is ascribed to the dynamic nature of the network; thermally activated reversible interactions (thermal dissociation/reformation of hydrogen bonds and disulfide exchange) allow chain mobility and network reorganization, enabling macroscopic flow at elevated temperature and efficient re-crosslinking on cooling. Together, these results demonstrate that PDDEGs can be fully recycled by simple, solvent-free heating while retaining its structure signature and mechanical performance, a desirable feature for sustainable materials.

Strong and durable adhesion is critical for practical sensing applications; accordingly, the adhesive behavior of PDDEGs was systematically evaluated. Qualitative tests (Fig. 4a) demonstrated that PDDEGs form conformal, robust contact with a wide range of substrates including glass, iron, wood, rubber, PET and Porcine skin, and skin-adhesion tests confirmed firm attachment with clean, residue-free removal (Fig. 4b). The combination of strong adhesion and inherent hydrophobicity also enables PDDEGs to function as an effective sealing tape for rapid hole repair and leak prevention (Fig. 4c). Quantitative lap-shear measurements (Figs. 4d–f) yielded bond strengths of 48 kPa for iron, 26 kPa for glass and 19 kPa for skin. Mechanistically, this performance reflects a synergistic interfacial chemistry: imidazolium cations and carboxyl groups within PDDEGs engage in hydrogen-bonding and coordination interactions with surface hydroxyl groups and metal ions, providing chemical anchoring and interfacial adhesion, while the hydrophobic fatty-acid backbone and long-chain imidazole modifications expel interfacial water and enhance van der Waals/hydrophobic contact, thereby stabilizing the bonding interface. The multivalent and dynamic nature of these interactions further promotes conformal contact and energy dissipation under stress, yielding durable adhesion across diverse environments.

$PDDEG_{2.5-0.05}$ exhibits good electrical conductivity, high ductility, and elasticity, enabling reliable strain-sensing performance. As shown in Fig. 5a, the gauge factors were 0.455, 0.714, and 0.995 in the strain ranges of 0–50%, 50%–100%, and 100%–200%, respectively. The $\Delta R/R_0$ signals remained highly repeatable over five consecutive cycles at both small strains of 1%–3% and large strains of 50%–200% (Fig. 5b). Moreover, $PDDEG_{2.5-0.05}$ displayed stable and consistent resistance responses at 50% strain across strain rates from 25 mm/min to 300 mm/min, indicating strain-rate-independent sensing (Fig. 5c). At a strain of 1%, the gel responded rapidly with a response time of approximately 0.4 s and a recovery time of approximately 0.8 s (Fig. 5d). Even after 300 cycles at 30% strain, the $\Delta R/R_0$ remained at about 20% (Fig. 5e), confirming excellent sensitivity, fast response, and long-term durability. Building on these favorable properties, $PDDEG_{2.5-0.05}$ was further applied to real-time monitoring of human motion (Figs. 5f–k). The sensor effectively tracked joint movements including those of the

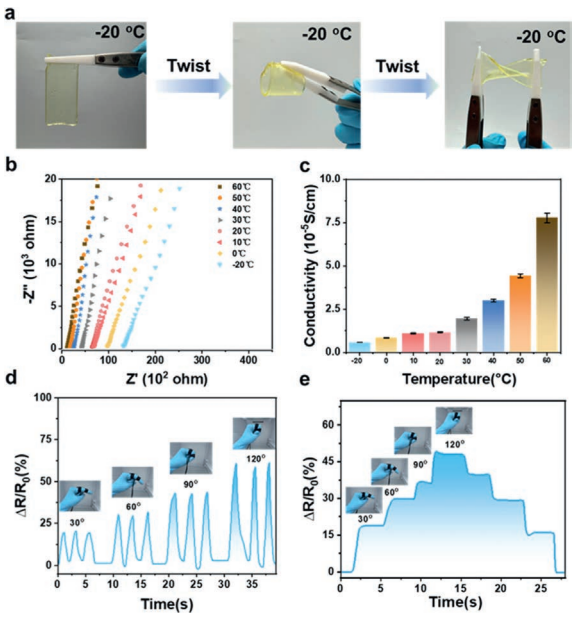


Fig. 6. (a) The extended sheets of PDDEG exhibited good flexibility at −20 °C. (b) Electrochemical impedance spectroscopy plots of $PDDEG_{2.5-0.05}$ under different temperature. (c) Ionic conductivities of $PDDEG_{2.5-0.05}$ under different temperature. (d, e) $PDDEG_{2.5-0.05}$ as a strain sensor for real-time monitoring of finger bending at different angles at −20 °C. Data are presented as mean ± SD ($n = 5$).

fingers, wrist, and elbow, producing stable and repeatable resistive responses when the joints were bent at fixed angles. It was also able to distinguish different degrees of finger bending, as $\Delta R/R_0$ increased progressively with the bending angle from 0 to 120 degrees, remained constant at fixed angles, and fully recovered when the finger was straightened, demonstrating outstanding reversibility. Beyond joint motion, $PDDEG_{2.5-0.05}$ successfully detected subtle facial expressions such as mouth opening (Fig. 5j) and even vocalization behavior, generating periodic resistance signals when attached to a volunteer's throat during repeated pronunciation of the word "Cool" (Fig. 5k). These results highlight the great potential of $PDDEG_{2.5-0.05}$ as a flexible, multifunctional sensor for real-time wearable applications at room temperature.

To further validate the low-temperature sensing performance of PDDEGs, we examined flexibility, mechanical properties, and electrical conductivity at reduced temperatures. As shown in Fig. 6a and Fig. S14 (Supporting information), $PDDEG_{2.5-0.05}$ remains highly flexible at −20 °C and even −40 °C; it can be bent and folded without fracture. Low-temperature tensile tests (Figs. S15–S17 in Supporting information) show that the tensile stress increases slightly from 62.7 kPa at 25 °C to 74.9 kPa at −20 °C, while the elongation at break decreases from 445.7 % to 360.1 %. Young's modulus rises modestly and the toughness is essentially unchanged. These results demonstrate that the material retains excellent mechanical integrity under subzero conditions. This excellent antifreeze performance is attributed to the DES matrix and the added inorganic ions. The DES disrupts regular chain packing and suppresses crystalline nucleation, which helps maintain an amorphous network and preserves segmental mobility at low temperature. The inorganic ions further inhibit crystallization. At the same time, ionic associations and hydrogen bonds become stronger at low temperature and act as reversible physical crosslinks. These interactions improve load transfer and thereby increase stress and modulus. Reduced mobility of dynamic bonds limits chain slippage and accounts for the decrease in elongation. Moreover, Table S5 (Supporting information) directly compares $PDDEG_{2.5-0.05}$ with representative low-temperature sensing gels recently reported in the literature. The results demonstrate that $PDDEG_{2.5-0.05}$ exhibits excellent overall performance, particularly in its self-healing ability and balanced mechanical strength and toughness at low temperatures. This excellent balance of properties highlights the unique advantages of PDDEG and its great potential for reliable application in low-temperature sensing environments.

Conductivity measurements (Figs. 6b and c, Fig S18 in Supporting information) showed that the conductivity decreases from 7.6×10^{-5} S/cm at 60 °C to 5.0×10^{-6} S/cm at −20 °C. The results show that the conductivity decreases with decreasing temperature, reflecting the slowing of polymer segment motion and the increased confinement of mobile ions, which limits ion transport. Nevertheless, the residual conductivity at low temperatures remains sufficient for sensing applications. As shown in Figs. 6d and e and Fig. S19 (Supporting information), $\Delta R/R_0$ increased steadily as the finger bending angle rose from 0° to 120°. Once the angle was fixed, $\Delta R/R_0$ remained stable. When the finger was straightened, $\Delta R/R_0$ returned completely to its initial value. These results confirm that $PDDEG_{2.5-0.05}$ maintains flexibility, conductivity, and reliable sensing performance even under subzero conditions.

In summary, we developed a new class of PDESs based on lipoic acid and imidazolium derivatives, which enabled the construction of recyclable PDDEGs. This molecular design integrates natural sustainability with high ionic mobility and antifreeze capacity. Through covalent crosslinking and reversible zirconium coordination, PDDEGs achieve a balanced combination of stretchability, toughness, and durable adhesion. More importantly, they exhibit outstanding recyclability, repeatable self-healing, and thermal remoldability, allowing solvent-free reprocessing, structural repair, and adaptive reshaping without performance loss. These dynamic properties ensure long service life and minimize material waste, addressing key sustainability challenges in wearable electronics. As strain sensors, PDDEGs show reliable conductivity, high sensitivity, and stable performance even at subzero temperatures. Overall, this work not only demonstrates the practical potential of PDDEGs in extreme-environment sensing, but also highlights polymerizable eutectic solvents as a general strategy to design multifunctional, sustainable gels for next-generation wearable devices.

CRediT authorship contribution statement

Yinzhou Guo: Writing – original draft, Funding acquisition, Formal analysis, Data curation, Conceptualization. **Yuanyuan Chen:** Software, Methodology, Formal analysis, Data curation. **Min Zhang:** Formal analysis, Data curation. **Chenhui Cui:** Software, Methodology, Funding acquisition, Formal analysis. **Xiaoqing Ming:** Software, Methodology, Formal analysis. **Zhang Qiang:** Validation, Methodology, Data curation. **Jiao Jiao:** Validation, Methodology. **Yilong Cheng:** Validation, Methodology. **Zhishen Ge:** Writing – review & editing, Validation. **Yanfeng Zhang:** Writing – review & editing, Methodology, Funding acquisition.

Declaration of competing interest

The authors declare that they have no known competing financial interests or personal relationships that could have appeared to influence the work reported in this paper.

Acknowledgments

The authors thank the Natural Science Basic Research Program of Shaanxi Province (No. 2024JC-YBQN-0448), the National Natural Science Foundation of China (NSFC, No. 52173079), the Fundamental Research Funds for the Central Universities (Nos. xtr052023001, xzy012023037), the Qin Chuangyuan High-level

Innovation and Entrepreneurship Talent Project (No. QCYRCXM-2022–139), the Qin Chuangyuan Scientists + Engineers Team Building Project of Shaanxi Province (No. 2022KXJ-108). The authors thank the Instrument Analysis Center of Xi'an Jiaotong University for the assistance with DSC and XRD analyses.

Supplementary materials

Supplementary material associated with this article can be found, in the online version, at doi:10.1016/j.cclet.2025.112122.

References

[1] S.W. Chen, Z. Qiao, Y. Niu, et al., Nat. Rev. Bioeng. 1 (2023) 950–971.
[2] Z.W. Zhang, B.F. Feng, J.P. Yan, et al., Green Chem. 27 (2025) 1604–1619.
[3] F.C. Zheng, H.Y. Jiang, X.T. Yang, et al., Chem. Eng. J. 490 (2024) 151874.
[4] Z.W. Lin, S.S. Duan, M.Y. Liu, et al., Adv. Mater. 36 (2024) 202306880.
[5] S. Nakata, M. Shiomi, Y. Fujita, et al., Nat. Electron. 1 (2018) 596–603.
[6] H. Jang, J. Lee, C.J. Beak, et al., Adv. Mater. 37 (2025) 202416073.
[7] X.J. Chen, Z.Z. Wan, R.H. Zhang, et al., Chem. Eng. J. 499 (2024) 156431.
[8] M.K. Li, Y.F. Zhang, L.S.Y. Lian, et al., Adv. Funct. Mater. 32 (2022) 202208141.
[9] Q. Zhang, Y. Wang, D.S. Li, et al., Adv. Funct. Mater. 33 (2023) 202209667.
[10] X.H. Zeng, Y. Lu, L.M. Zou, et al., Chem. Eng. J. 510 (2025) 161566.
[11] Z.J. Zhao, X. Fan, S.X. Wang, et al., Chin. Chem. Lett. 34 (2023) 107892.
[12] H.M. Lin, D.D. Zheng, X.L. Wu, et al., Sci. Adv. 10 (2024) 0730.
[13] P.F. Xu, S.J. Wang, A. Lin, et al., Nat. Commun. 14 (2023) 623.
[14] B. Yiming, S. Hubert, A. Cartier, et al., Nat. Commun. 16 (2025) 431.
[15] X.S. Pan, J. Li, N. Ma, et al., Chem. Eng. J. 461 (2023) 142062.
[16] H. Zhang, D.Z. Zhang, H.L. Cai, et al., Carbohydr. Polym. 360 (2025) 123601.
[17] T.K.N. Duong, T.T. Truong, T.N.L. Phan, et al., Aggregate 6 (2025) 70047.
[18] Y.Y. Shi, C.C. Liu, Z.J. Zuo, et al., Chin. Chem. Lett. 36 (2025) 109772.
[19] X.H. Cui, Y.B. Xi, S.W. Tu, et al., TrAC Trend Anal. Chem. 174 (2024) 117662.
[20] S. Wang, J.L. Ning, J.Y. Pu, et al., Nano Mater. Sci. 7 (2025) 316–325.
[21] Y.H. Zhou, X. Fei, J. Tian, et al., Colloid Interface Sci 606 (2022) 192–203.
[22] D.K. Yu, D.P. Jiang, Z.M. Xue, et al., Green Chem. 26 (2024) 7478–7507.
[23] M.R. Rabiei, M. Hosseini, G.B. Xu, Microchem. J. 203 (2024) 110909.
[24] A. Prabhune, R. Dey, J. Mol. Liq. 379 (2023) 121676.
[25] H.H. Xiong, Y.Q. Wan, Y. Fan, et al., Chin. Chem. Lett. 35 (2024) 108382.
[26] J.Y. Zhang, S. Li, L.P. Yao, et al., Chin. Chem. Lett. 34 (2023) 107750.
[27] T.Y. Chen, Y.J. Jiang, H.W. Chien, Polymers 15 (2023) 2605.
[28] M. Sang, J.J. Wang, D.Y. Zuo, et al., ACS Sustain. Chem. Eng. 12 (2024) 2455–2464.
[29] T. Huang, Y.B. Zhang, L. Zhao, et al., Int. J. Biol. Macromol. 257 (2024) 128801.
[30] J.T. Li, M.Z. Zhang, J.L. He, et al., Chem. Commun. 59 (2023) 8814–8817.
[31] Y. Tian, F. Jiang, H.J. Xie, et al., Adv. Healthc. Mater. 13 (2024) 202304117.
[32] K.X. Yu, Y.F. Gao, R. Wang, et al., Macromol. Rapid. Commun. 45 (2024) 202300557.
[33] P.Q. Yao, Q.W. Bao, Y. Yao, et al., Adv. Mater. 35 (2023) 202300114.
[34] X.J. Liu, J.B. Wang, P.F. Lv, et al., Energy Stor. Mater 69 (2024) 103382.
[35] X.J. Zhang, S. Liu, X.B. Wang, et al., J. Colloid Interface Sci. 654 (2024) 1348–1355.
[36] L. Lin, R.A. Li, G.X. Chen, et al., Polym. Chem. 15 (2024) 783–795.
[37] Y.H. Zhang, L. Jiang, H.B. Zhang, et al., Molecules 28 (2023) 4690.
[38] W.K. Xu, T. Shen, Y.T. Ding, et al., Small 20 (2024) 202310072.